

Constraints on large- x parton distributions from new weak boson production and deep-inelastic scattering data

A. Accardi,^{1,2} L. T. Brady,^{2,3} W. Melnitchouk,² J. F. Owens,⁴ and N. Sato²

¹*Hampton University, Hampton, Virginia 23668, USA*

²*Jefferson Lab, Newport News, Virginia 23606, USA*

³*University of California, Santa Barbara, California 93106, USA*

⁴*Florida State University, Tallahassee, Florida 32306, USA*

(Received 15 February 2016; published 20 June 2016)

We present a new set of leading-twist parton distribution functions, referred to as “CJ15,” which take advantage of developments in the theoretical treatment of nuclear corrections as well as new data. The analysis includes, for the first time, data on the free neutron structure function from Jefferson Lab and new high-precision charged lepton and W -boson asymmetry data from Fermilab. These significantly reduce the uncertainty on the d/u ratio at large values of x and provide new insights into the partonic structure of bound nucleons.

DOI: [10.1103/PhysRevD.93.114017](https://doi.org/10.1103/PhysRevD.93.114017)

I. INTRODUCTION

Tremendous advances have been made over the past decade in our knowledge of the quark and gluon (or parton) substructure of the nucleon, with the availability of new high-energy scattering data from various accelerator facilities worldwide [1–3]. Results from the final analysis of data from the ep collider HERA have allowed a detailed mapping of the partonic landscape at small values of the nucleon’s parton momentum fraction x [4]. Data from high-energy $p\bar{p}$ scattering at the Tevatron on weak boson and jet production have provided a wealth of complementary information on the nucleon’s flavor structure. At lower energies, precision structure function measurements at the high-luminosity CEBAF accelerator at Jefferson Lab have enabled a detailed investigation of nucleon structure at large values of x [5]. More recently, fascinating glimpses into the role played by sea quarks and gluons in the proton have been seen in various channels in pp collisions at the LHC.

To analyze the vast amounts of data from the various facilities, concerted efforts are being made to systematically extract information about the nucleon’s quark and gluon structure in the form of parton distribution functions (PDFs) [6–14]. While much of the effort has in the past been directed at the small- x frontier made accessible through the highest-energy colliders, relatively less attention has been focused on the region of large momentum fractions, where nonperturbative QCD effects generally play a more important role.

The CTEQ-Jefferson Lab (CJ) Collaboration [15] has performed a series of global PDF analyses [12–14] with the aim of maximally utilizing data at the highest- x values amenable to perturbative QCD treatment. The additional complications of working with data down to relatively low values of four-momentum transfer Q^2 ($Q^2 \gtrsim 1\text{--}2\text{ GeV}^2$)

and invariant final state masses W^2 ($W^2 \gtrsim 4\text{ GeV}^2$) have been met with developments in the theoretical description of various effects which come into prominence at such kinematics. The importance of $1/Q^2$ power corrections, arising from target mass and higher-twist effects, has been emphasized [12,13] particularly in the analysis of fixed-target deep-inelastic scattering (DIS) data, which found leading-twist PDFs to be stable down to low- Q^2 values with the inclusion of both of these effects.

Moreover, since the CJ analyses typically fit both proton and deuterium data, the description of the latter requires careful treatment of nuclear corrections at large values of x , at all Q^2 scales. The d -quark PDF is especially sensitive to the deuterium corrections for $x \gtrsim 0.5$, and historically has suffered from large uncertainties due to the model dependence of the nuclear effects [16]. To adequately allow for the full range of nuclear model uncertainties, the CJ12 analysis [14] produced three sets of PDFs corresponding to different strengths (minimum, medium and maximum) of the nuclear effects, which served to provide a more realistic estimate of the d -quark PDF uncertainty compared with previous fits.

In this analysis, which we refer to as “CJ15,” we examine the impact of new large rapidity charged lepton and W -boson asymmetry data from the Tevatron [17–19] on the determination of next-to-leading-order (NLO) PDFs and their errors, particularly at large values of x . We also include for the first time new Jefferson Lab data on the free neutron structure function obtained from backward spectator proton tagging in semi-inclusive DIS [20,21], which do not suffer from the same uncertainties that have afflicted previous neutron extractions. We present a more complete treatment of the nuclear corrections in deuterium, examining a range of high-precision deuteron wave functions and several models for the nucleon off-shell corrections. In contrast to our earlier fits [12–14], which relied on

and the deuteron wave function, defining a set of nuclear corrections that ranged from mild (for the hardest, WJC-1 wave function [70] coupled to a small, 0.3% nucleon swelling) to strong (for the softest, CD-Bonn wave function [69] with a large, 2.1% swelling parameter). The entire range of nuclear corrections was consistent with the existing experimental data, with each of the CJ12min, CJ12mid and CJ12max PDF sets giving essentially the same χ^2 values for the global fit, $\chi^2/\text{datum} \approx 1.03$.

In the present CJ15 analysis, in order to decrease the model dependence of the off-shell correction and increase the flexibility of the fit, we follow the proposal of Kulagin and Petti [66] and employ a phenomenological parametrization with parameters fitted to data. From the constraint that the off-shell correction does not modify the number of valence quarks in the nucleon,

$$\int_0^1 dx \delta f^N(x) [q(x) - \bar{q}(x)] = 0, \quad (14)$$

one can infer that the function δf^N must have one or more zeros in the physical range between $x = 0$ and 1. We can, therefore, take the off-shell function δf^N to be parametrized by the form

$$\delta f^N = C(x - x_0)(x - x_1)(1 + x_0 - x), \quad (15)$$

with the zeros x_0 and x_1 and normalization C free parameters. In practice, we fit the zero crossing parameter x_0 and the normalization C , which then allows the second zero crossing x_1 to be determined from Eq. (14) analytically. In Ref. [66], these parameters were constrained by fitting to ratios of nuclear to deuteron structure function data, for a range of nuclei up to ^{207}Pb . This resulted in a combined nuclear correction that produced a ratio of deuteron to nucleon structure functions F_2^d/F_2^N with a shape similar to that for heavy nuclei [78,79], including an $\approx 1\%$ antishadowing enhancement in F_2^d/F_2^N at $x \approx 0.1$ – 0.2 . In contrast, in the present analysis, we fit the off-shell parameters by considering only deuteron cross section data and their interplay with proton data for a range of processes sensitive to the d -quark PDF.

To test the sensitivity of the fit to the off-shell parametrization, we also consider as an alternative the model of Ehlers *et al.* [64], who generalized the quark spectator model employed in the CJ12 analysis [14] to allow for different off-shell behaviors of the valence quark, sea quark and gluon distributions. In previous studies the off-shell corrections were implemented only for the deuteron F_2^d structure function and in the valence quark approximation. The generalized model [64], on the other hand, which we refer to as the “off-shell covariant spectator” (OCS) model, can be applied to observables that are sensitive to both the valence and sea sectors, such as the deuteron F_L^d structure function or proton–deuteron Drell-Yan cross sections.

More specifically, in the OCS model, three masses for the respective spectator states (“ qq ” for valence quarks, “ $qq\bar{q}q$ ” for sea quarks, and “ qqq ” for gluons) were fitted to the isoscalar valence, sea quark and gluon PDFs in the free nucleon. The only free parameter in the model is the rescaling parameter $\lambda = \partial \log \Lambda^2 / \partial \log p^2$, evaluated at $p^2 = M^2$. The variable λ can then be included as a parameter in the fit, with errors propagated along with those of the other leading-twist parameters.

Finally, we note that in a purely phenomenological approach adopted by Martin *et al.* [80], the entire deuteron nuclear correction is parametrized by a Q^2 -independent function, without appealing to physical constraints. To mock up the effects of Fermi motion, the parametrization includes a logarithm raised to a high power, $\sim \ln^{20}(x)$, which produces the steep rise in the F_2^d/F_2^N ratio at high x . In the convolution formula in Eq. (9), this effect arises naturally from the smearing of the nucleon structure function by the nucleon momentum distribution function $f_{N/d}$.

III. DATA

The CJ15 PDFs are obtained by fitting to a global database of over 4500 data points from a variety of high-energy scattering processes, listed in Table I. These include deep-inelastic scattering data from BCDMS [81], SLAC [82], NMC [83,84], HERA [85], HERMES [86] and Jefferson Lab [20,21,87], Drell-Yan pp and pd cross sections from fixed target experiments at Fermilab [29], W [17–19,88,89] and Z [90,91] asymmetries, as well as jet [92,93] and γ + jet [94] cross sections from the CDF and DØ Collaborations at the Tevatron. Cuts on the kinematic coverage of the DIS data have been made for $Q^2 > Q_0^2 = 1.69 \text{ GeV}^2$ and $W^2 > 3 \text{ GeV}^2$, as in the CJ12 analysis [14]. Compared with the CJ12 fit, however, several new data sets are included in the new analysis.

For DIS, we include the new results from the BONuS experiment [20,21] in Jefferson Lab’s Hall B, which collected around 200 data points on the ratio of neutron to deuteron F_2 structure functions up to $x \approx 0.6$, using a spectator tagging technique to isolate DIS events from a nearly free neutron inside a deuteron nucleus [75]. Unlike all previous extractions of neutron structure from deuteron targets, which have been subject to large uncertainties in the nuclear corrections in the deuteron at high x [16,67], the BONuS data provide the first direct determination of F_2^n in the DIS region, essentially free of nuclear uncertainties.

New data sets from the run II of HERA [4,85] and from HERMES on the proton and deuteron structure functions [86] have become available recently, and are included in this analysis. During the fitting process it was noted that the HERMES data from the highest- Q^2 bin (bin “F” [86]) differed significantly from results from other experiments in the same kinematic region, and in the final analysis the

TABLE I. Data sets used in the CJ15 global analysis, with the corresponding number of data points and χ^2 values for each set. The main CJ15 NLO fit (in boldface), which uses the AV18 deuteron wave function and off-shell parametrization in Eq. (15), is compared with an LO fit and NLO fits with the OCS off-shell model, no nuclear corrections, and no nuclear corrections or DØ W asymmetry data.

Observable	Experiment	# points	χ^2				
			LO	NLO	NLO (OCS)	NLO (no nucl)	NLO (no nucl/DØ)
DIS F_2	BCDMS (p) [81]	351	426	438	436	440	427
	BCDMS (d) [81]	254	292	292	289	301	301
	SLAC (p) [82]	564	480	434	435	441	440
	SLAC (d) [82]	582	415	376	380	507	466
	NMC (p) [83]	275	416	405	404	405	403
	NMC (d/p) [84]	189	181	172	173	174	173
	HERMES (p) [86]	37	57	42	43	44	44
	HERMES (d) [86]	37	52	37	38	36	37
	Jefferson Lab (p) [87]	136	172	166	167	177	166
	Jefferson Lab (d) [87]	136	131	123	124	126	130
DIS F_2 tagged	Jefferson Lab (n/d) [21]	191	216	214	213	219	219
DIS σ	HERA (NC e^-p) [85]	159	315	241	240	247	244
	HERA (NC e^+p 1) [85]	402	952	580	579	588	585
	HERA (NC e^+p 2) [85]	75	177	94	94	94	93
	HERA (NC e^+p 3) [85]	259	311	249	249	248	248
	HERA (NC e^+p 4) [85]	209	352	228	228	228	228
	HERA (CC e^-p) [85]	42	42	48	48	45	49
	HERA (CC e^+p) [85]	39	53	50	50	51	51
Drell-Yan	E866 (pp) [29]	121	148	139	139	145	143
	E866 (pd) [29]	129	202	145	143	158	157
W /charge asymmetry	CDF (e) [88]	11	11	12	12	13	14
	DØ (μ) [17]	10	18	20	19	29	28
	DØ (e) [18]	13	49	29	29	14	14
	CDF (W) [89]	13	16	16	16	14	14
	DØ (W) [19]	14	35	14	15	82	—
Z rapidity	CDF (Z) [90]	28	108	27	27	26	26
	DØ (Z) [91]	28	26	16	16	16	16
jet	CDF (run 2) [92]	72	29	15	15	23	25
	DØ (run 2) [93]	110	87	21	21	14	14
γ + jet	DØ 1 [94]	16	16	7	7	7	7
	DØ 2 [94]	16	34	16	16	17	17
	DØ 3 [94]	12	35	25	25	24	25
	DØ 4 [94]	12	79	13	13	13	13
total		4542	5935	4700	4702	4964	4817
total + norm			6058	4708	4710	4972	4826
χ^2 /datum			1.33	1.04	1.04	1.09	1.07

data in the Q^2 bin F were not included. The other DIS data sets are unchanged from those used in the CJ12 analysis [14].

For the Drell-Yan data from the E866 experiment [29] at Fermilab, following the suggestion in Ref. [95] we employ a cut on the dimuon cross sections for dimuon masses $M_{\mu^+\mu^-} > 6$ GeV. This reduces the number of data points from 375 to 250 compared to the usual cut of $M_{\mu^+\mu^-} \gtrsim 4$ GeV, but leads to a significant reduction in the χ^2 /datum for those data. In previous fits, dimuon data from the E605 Drell-Yan experiment at Fermilab [96] were also used. However, those data were taken on a copper target and are therefore potentially subject to nuclear corrections. Since the nuclear corrections used in the

CJ15 fit pertain only to deuterium targets, we have chosen not to use the E605 data in this analysis.

Several new data sets from W -boson production in pp collisions at the Tevatron have also recently become available and are included in the CJ15 fit. New data from the DØ Collaboration on muon [17] and electron [18] charge asymmetries supersede previous lepton asymmetry measurements, and remove the tension with the extracted W -boson asymmetries that was evident in our previous CJ12 analysis [14]. The new W -boson asymmetry data from DØ [19] have about 10 times larger integrated luminosity, and extend over a larger W -boson rapidity range, up to ≈ 3 , than the earlier CDF measurement [89]. While the lepton asymmetry data are more sensitive to

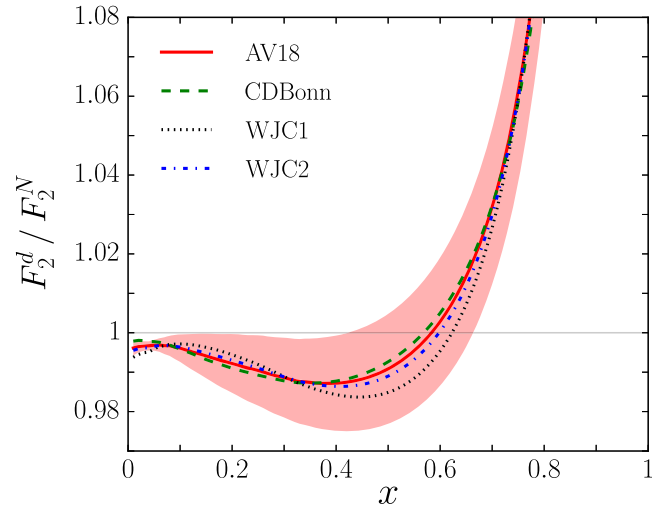


FIG. 9. Ratio of deuteron to isoscalar nucleon structure functions F_2^d/F_2^N for different deuteron wave function models at $Q^2 = 10 \text{ GeV}^2$: AV18 (solid red curve with 90% C.L. uncertainty band), CD-Bonn (dashed green curve), WJC-1 (dotted black curve) and WJC-2 (dot-dashed blue curve).

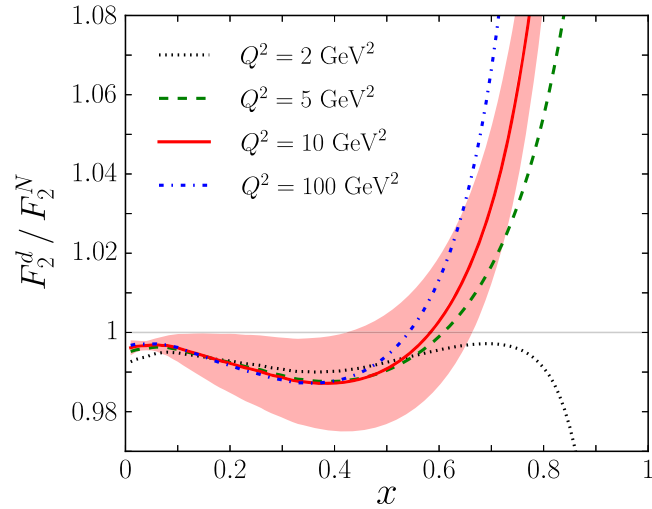


FIG. 10. Ratio of deuteron to isoscalar nucleon structure functions F_2^d/F_2^N computed from the CJ15 PDFs for different values of Q^2 : 2 GeV^2 (dotted black curve), 5 GeV^2 (dashed green curve), 10 GeV^2 (solid red curve with 90% C.L. uncertainty band) and 100 GeV^2 (dot-dashed blue curve).

together with earlier data from CDF [88], are displayed in Fig. 12 as a function of the lepton pseudorapidity η_ℓ and compared with the CJ15 fit. The extracted W boson asymmetries, which are more directly related to the shape of the PDFs and are not limited in their x reach by the lepton decay vertex smearing, are shown in Fig. 13 as a function of the W boson rapidity y_W . The statistical errors on the DØ data in particular are extremely small and place strong constraints on the fit. The earlier CDF electron and

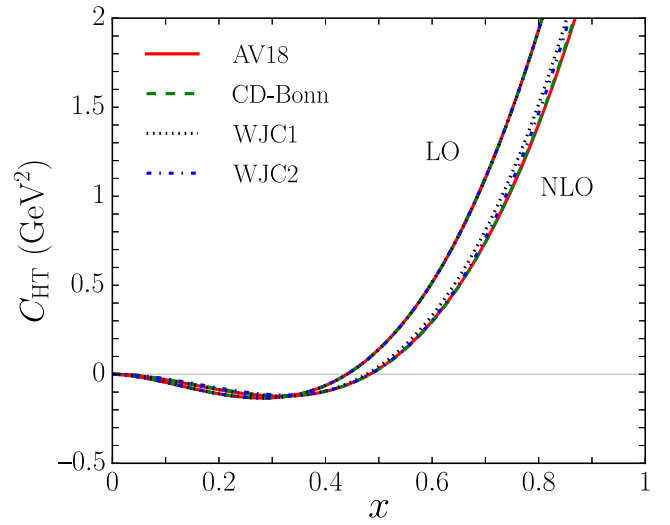


FIG. 11. Fitted higher twist function C_{HT} from Eq. (8), in units of GeV^2 , for different deuteron wave function models. The higher twist term for the CJ15 NLO fit is compared with the corresponding term in the LO fit. The 90% C.L. uncertainty band is barely visible and is not shown here.

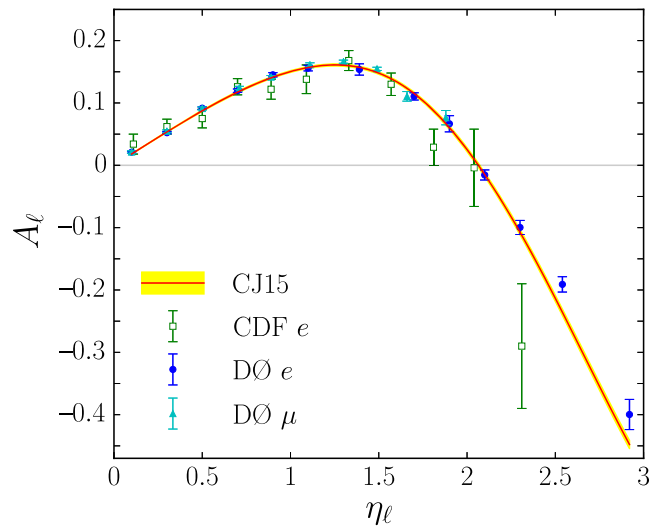


FIG. 12. Lepton charge asymmetry A_ℓ from $p\bar{p} \rightarrow WX \rightarrow \ell\nu X$ as a function of the lepton pseudorapidity η_ℓ from CDF electron (green open squares) [88], DØ electron (blue circles) [18] and DØ muon (cyan triangles) [17] data compared with the CJ15 fit with 90% C.L. uncertainty (yellow band).

W data have larger errors and have more limited constraining power. Compared with the range of nuclear corrections in CJ12, the asymmetry data, and especially the new results from DØ, strongly favor smaller nuclear corrections at large x , closer to those in the CJ12min set.

The stronger constraints from the lepton and W charge asymmetry data lead to a significant reduction in the uncertainties on the d/u ratio, particularly at large values

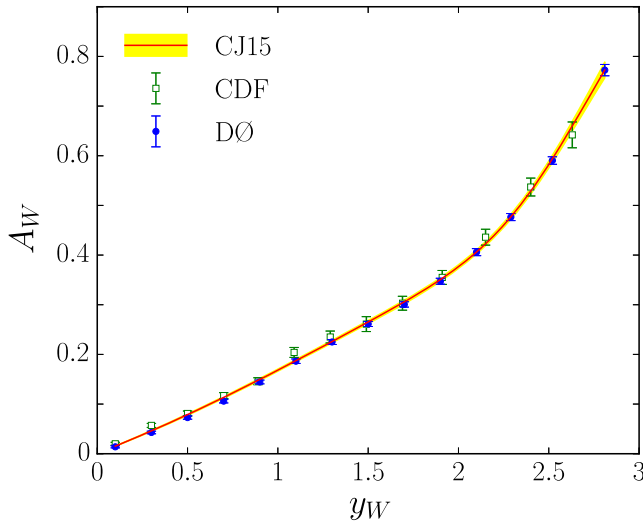


FIG. 13. W boson charge asymmetry A_W from $p\bar{p} \rightarrow WX$ as a function of the W boson rapidity y_W for CDF (green open squares) [89] and DØ (blue circles) [19] data compared with the CJ15 fit with 90% C.L. uncertainty (yellow band).

of x . This is illustrated in Fig. 14, which demonstrates the shrinking of the d/u uncertainty bands (which are shown here and in the remainder of this section at the 90% C.L.) with the successive addition of various data sets. Compared with the fit to DIS only data, in which the d/u ratio has very large uncertainties beyond $x \approx 0.4$, the addition of the lepton asymmetries leads to a reduction in d/u of more than a factor of two at $x \lesssim 0.4$, with more limited impact at

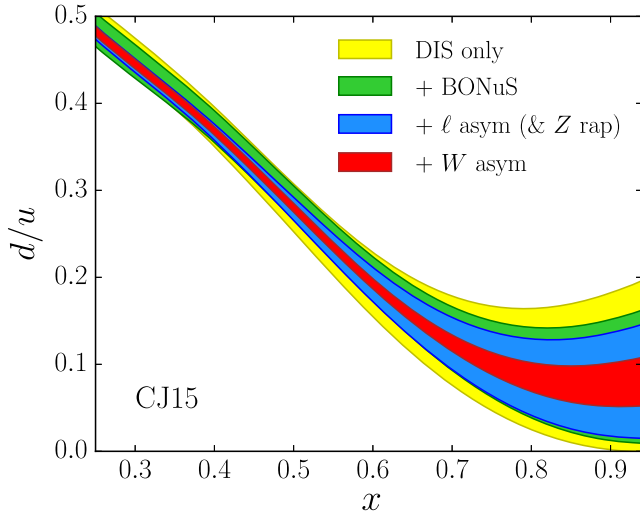


FIG. 14. Impact of various data sets on the d/u ratio at $Q^2 = 10 \text{ GeV}^2$. The 90% C.L. uncertainty band is largest for the DIS only data (yellow band), and decreases with the successive addition of Jefferson Lab BONuS F_2^n/F_2^d [21] data (green band), lepton asymmetry [17,18,88] (and Z rapidity [90,91]) data (blue band), and W boson asymmetry data [19,89] (red band).

higher- x values due to the PDF smearing caused by the lepton decay vertex. (Addition of Z boson rapidity data [90,91] has only modest impact on d/u .) Subsequent inclusion of the W asymmetries leads to a further halving of the uncertainty at $x \approx 0.6$ – 0.8 , while having minimal effect on the errors at $x \lesssim 0.4$.

In fact, independent of the charge asymmetry data, a significant reduction in the d/u uncertainty at intermediate x values is already provided by the Jefferson Lab BONuS data on F_2^n/F_2^d [20,21]. While the BONuS data have little or no effect at $x \lesssim 0.3$, the reduction in the d/u error at $x \sim 0.5$ – 0.6 is almost as large as that from the lepton asymmetries. (The BONuS data have a slight preference for stronger nuclear corrections, in contrast to the lepton asymmetry data, although the tension is not significant.) Using all the available data from DIS and W boson production, the central value of the extrapolated d/u ratio at $x = 1$ is ≈ 0.1 at the input scale Q_0^2 . The nuclear model dependence of the central values of the $x \rightarrow 1$ limit of d/u is relatively weak, ranging from 0.08 for the WJC-1 wave function to 0.12 for the CD-Bonn model. For our best fit, we obtain the extrapolated value,

$$d/u \xrightarrow{x \rightarrow 1} 0.09 \pm 0.03, \quad (16)$$

at the 90% C.L., which represents a factor ≈ 2 reduction in the central value compared with the CJ12 result [14].

While the new charge asymmetry and BONuS F_2^n/F_2^d measurements provide important constraints on the d/u ratio, the existing inclusive deuteron DIS data still play an important role in global analyses, as does the proper treatment of the nuclear corrections. If one were to fit F_2^d data without accounting for nuclear effects (assuming $F_2^d = F_2^p + F_2^n$), the resulting d/u ratio would be strongly overestimated beyond $x = 0.6$, where the F_2^d/F_2^N ratio begins to deviate significantly from unity (see Fig. 9). This is illustrated in Fig. 15, where the CJ15 d/u ratio is compared with the fit without nuclear corrections. This behavior can be understood from the shape of the F_2^d/F_2^N ratio Fig. 9 at large x , where the effect of the nuclear corrections is to increase the ratio above unity for $x \gtrsim 0.6$. Since F_2^d and F_2^p are fixed inputs, a larger F_2^d/F_2^N is generated by a smaller neutron F_2^n and hence a smaller d/u ratio. For example, the effect of the nuclear corrections is to shift the d/u ratio at $x = 0.8$ from the range ≈ 0.1 – 0.3 to ≈ 0 – 0.2 once the smearing and off-shell effects are included. Removing the deuterium data altogether increases the overall uncertainty band for $x \gtrsim 0.7$. The deuteron data also reduce the d/u uncertainties slightly at smaller values of $x \lesssim 0.2$ (see below).

Effects on large- x PDFs from nuclear corrections have also been investigated by several other groups in recent years [6,10,80,99,106] and it is instructive to compare the CJ15 results on the d/u ratio with those analyses.

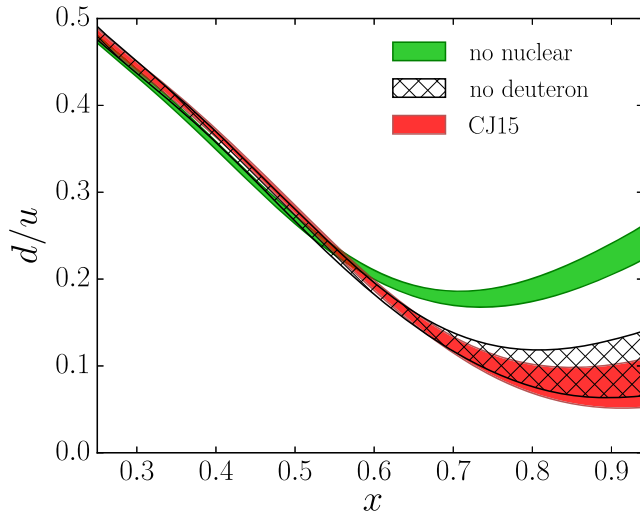


FIG. 15. Impact on the CJ15 d/u ratio at $Q^2 = 10 \text{ GeV}^2$ (red band) of removing the deuterium nuclear corrections (green band), and omitting the deuterium data (cross-hatched band).

The MMHT14 fit [6] uses a purely phenomenological, Q^2 -independent nuclear correction for the combined effects of nuclear smearing and off-shell corrections, in contrast to our approach in which the (poorly understood) off-shell correction is fitted, but the (better known) deuteron wave function correction is computed, and finite- Q^2 effects are taken into account. Interestingly, the phenomenological MMHT14 F_2^d/F_2^N ratio has a qualitatively similar shape to that found in our more microscopic estimate, which offers an important cross check of our formalism. For $x \lesssim 0.7$, the MMHT14 d/u uncertainty is comparable to that in CJ15, although for $x \gtrsim 0.8$ the uncertainty diverges rapidly due to the adoption of a stiffer d -quark parametrization, which only allows the d/u ratio to approach zero or infinity as $x \rightarrow 1$.

The JR14 analysis [10] uses similar smearing functions to those used in our fit, but does not include nucleon off-shell corrections. Furthermore, it uses the $\Delta\chi^2 = 1$ criterion for the 1σ C.L., based on statistical considerations alone, introducing additional systematic uncertainties through the dependence of the fit on the input scale. The resulting uncertainty on d/u is larger than that in CJ15 in the intermediate- x region, which may reflect the absence of the recent W and lepton asymmetry data in the JR14 fit. The range of d/u values extrapolated to $x = 1$ is similar to the CJ15 band within errors, although the form of the JR14 parametrization forces $d/u \rightarrow 0$ at $x = 1$.

The CJ15 uncertainty band in Fig. 16 is also similar to that found in the CT14 global analysis [7], which does not apply any nuclear corrections to deuterium data, on the basis of the somewhat higher W^2 cuts utilized. The CT14 analysis uses a parametrization based on Bernstein polynomials multiplying a common factor $x^{a_1}(1-x)^{a_2}$, and fixes the exponents a_2 to be the same for the u - and d -quark

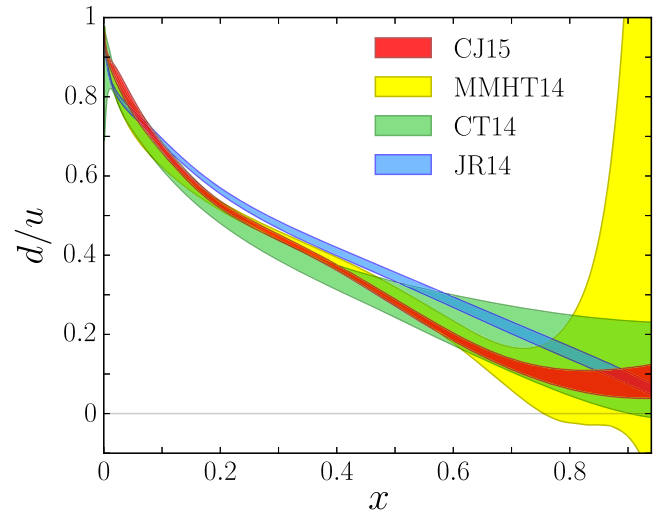


FIG. 16. Comparison of the d/u ratio at $Q^2 = 10 \text{ GeV}^2$ for different PDF parametrizations: CJ15 (red band), MMHT14 [6] (yellow band, 68% C.L.), CT14 [7] (green band), and JR14 [10] (blue band, scaled by a factor 1.645 for the 90% C.L.).

PDFs, thereby allowing finite values of the d/u ratio in the $x \rightarrow 1$ limit. The results of the two analyses largely overlap over much of the x range, with the CT14 distributions being slightly above the CJ15 error band at $x \gtrsim 0.6$. This is reminiscent of the higher d/u ratio observed in Fig. 15 when the nuclear corrections are switched off.

Finally, in Fig. 17 we show the d/u uncertainty from the CJ15 fit compared with the uncertainties obtained in fits excluding DIS deuteron or W asymmetry data. The W asymmetry data, which are statistically dominated by the

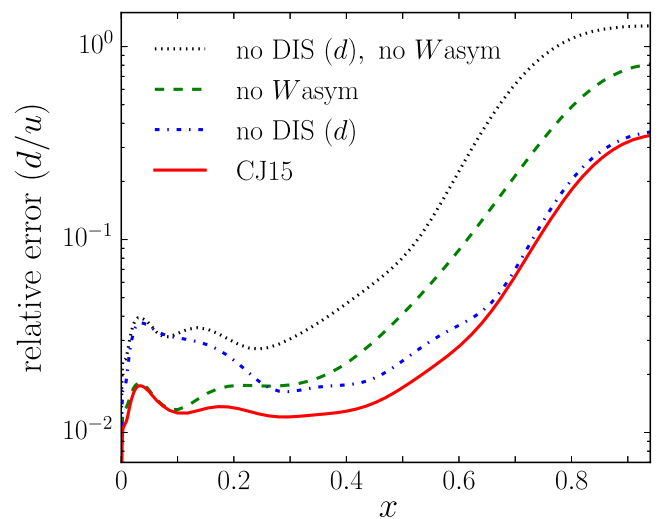


FIG. 17. Relative error on the d/u PDF ratio versus x at $Q^2 = 10 \text{ GeV}^2$ from the CJ15 fit (90% C.L., solid red curve) compared with the uncertainties obtained in fits excluding deuteron DIS data (dot-dashed blue curve) or W asymmetry data (dashed green curve), as well as excluding both (dotted black curve).

DØ results, provide the main constraint on the d/u ratio at $x \gtrsim 0.3$. At $x \lesssim 0.3$, where the statistical power of the reconstructed W asymmetry data becomes limited, the global deuteron DIS data play a vital role in reducing the uncertainty in the d/u ratio by more than 50%. At $x \gtrsim 0.6$, the statistical power of the DIS data is utilized instead to fit the off-shell function δf^N . The combination of these two observables provides a good illustration of the complementarity of different data sets in global fits in constraining PDFs over extended regions of x .

V. CONCLUSION

We have presented here results of the CJ15 global NLO analysis of parton distributions, taking into account the latest developments in theory and the availability of new data. Focusing particularly, but not exclusively, on the large- x region, the new analysis features a more comprehensive treatment of nuclear corrections to deuterium data, as well as a more flexible parametrization of the SU(2) light antiquark asymmetry, and an improved treatment of heavy quarks. In contrast to the earlier CJ12 fit [14], which used physically motivated models for the nucleon off-shell corrections, the present analysis allows the magnitude and shape of the off-shell effects to be phenomenologically constrained directly from data.

Along with the expanded set of proton and deuteron DIS data afforded by our less restrictive kinematic cuts $Q^2 > (1.3 \text{ GeV})^2$ and $W^2 > 3 \text{ GeV}^2$, we also include new results from the BONuS experiment at Jefferson Lab [20,21], which provide the first determination of the neutron structure function essentially free of nuclear correction uncertainties. The greatest impact on the fits, however, comes from the new DØ W asymmetry data at large rapidity [19], which because of their high precision and kinematic reach are able to place significant constraints on PDFs at high x . In particular, while the previous CJ12 analysis provided three sets of PDFs corresponding to a range of different deuterium and off-shell models, the new W asymmetry data strongly favor models with smaller nuclear corrections, closer to the “CJ12min” PDF set [14]. Within the parametrization of the nucleon off-shell corrections adopted here, our analysis has a slight preference for deuteron wave functions with softer momentum distributions, but essentially indistinguishable fits can be obtained with each of the deuteron models considered.

Our approach to the nuclear corrections is similar in spirit to the phenomenological analysis of Ref. [66], which makes use of DIS data on a wide range of nuclear targets and finds the ratio F_2^d/F_2^N to have a universal shape similar to that for F_2^A/F_2^d for heavy nuclei. From the proton and deuterium data alone, however, we find no evidence for an enhancement of F_2^d/F_2^N in the vicinity of $x \approx 0.1$. The only way to definitively resolve this question may be with data on the free neutron structure function that are not subject to

assumptions about nuclear corrections in deuterium. The phenomenological approach of fitting the nuclear effects directly was also utilized in Refs. [6,80], who parametrized the entire nuclear correction by a function that mimics both the effects of the smearing and the nucleon off-shell correction. Since the nuclear physics of the deuteron at long distances is relatively well understood, our philosophy is to include in the theoretical description the effects that can be computed reliably, and parametrize those that are more strongly model dependent.

As anticipated in Refs. [14,23] and elaborated in Ref. [104], the new precision measurements of observables that are sensitive to the d -quark PDF, but less sensitive to nuclear corrections, are seen to play an important role in allowing global QCD fits to constrain models of nuclear corrections in the deuteron. In particular, a simultaneous fit of the new W charge asymmetries [19] and the SLAC deuteron DIS structure functions [82] is only possible when nuclear corrections are taken into account. The interplay of these two data sets within the CJ15 fit has provided the first determination of nucleon off-shell effects in quark distributions in the deuteron within a global QCD context. At the same time, the d/u ratio has seen a significant reduction in its uncertainty at $x \gtrsim 0.5$, with an extrapolated central value ≈ 0.1 at $x \rightarrow 1$, or about half of that found in the CJ12 fit [14]. As discussed in Refs. [107,108], a precise determination of the d -quark PDF at large x is vital for searches for physics beyond the standard model at the LHC at the edges of kinematics, such as at large rapidities in heavy weak-boson production or, more generally, in large invariant mass observables.

The uncertainty in the d/u ratio is expected to be further reduced once new data from experiments at the energy-upgraded Jefferson Lab facility become available [101–103], that will probe PDFs up to $x \sim 0.85$ at DIS kinematics. The first of these, involving the simultaneous measurement of inclusive DIS cross section from ^3He and ^3H [101], in which the nuclear corrections are expected to mostly cancel [109–112], is scheduled to begin data taking in Fall 2016. The current analysis provides a timely benchmark against which the upcoming experimental results can be calibrated.

ACKNOWLEDGMENTS

We thank E. Christy, C. Keppel, P. Monaghan and S. Malace for their collaboration and assistance with the experimental data sets and S. Kulagin and R. Petti for helpful discussions. This work was supported by the DOE Contract No. DE-AC05-06OR23177, under which Jefferson Science Associates, LLC operates Jefferson Lab. The work of J. F. O. and A. A. was supported in part by DOE Contracts No. DE-FG02-97ER41922 and No. DE-SC0008791, respectively.

- [1] P. Jimenez-Delgado, W. Melnitchouk, and J. F. Owens, *J. Phys. G* **40**, 093102 (2013).
- [2] J. Blümlein, *Prog. Part. Nucl. Phys.* **69**, 28 (2013).
- [3] S. Forte and G. Watt, *Annu. Rev. Nucl. Part. Sci.* **63**, 291 (2013).
- [4] A. M. Cooper-Sarkar, *Proc. Sci., DIS2015* (2015) 005, [arXiv:1507.03849](https://arxiv.org/abs/1507.03849).
- [5] M. E. Christy and W. Melnitchouk, *J. Phys. Conf. Ser.* **299**, 012004 (2011).
- [6] L. A. Harland-Lang, A. D. Martin, P. Motylinski, and R. S. Thorne, *Eur. Phys. J. C* **75**, 204 (2015).
- [7] S. Dulat, T.-J. Hou, J. Gao, M. Guzzi, J. Huston, P. Nadolsky, J. Pumplin, C. Schmidt, D. Stump, and C.-P. Yuan, *Phys. Rev. D* **93**, 033006 (2016).
- [8] R. D. Ball *et al.*, *J. High Energy Phys.* **04** (2015) 040.
- [9] V. Radescu, in *Proceedings of 35th International Conference of High Energy Physics (ICHEP2010)*, Paris, France (2010), [arXiv:1308.0374](https://arxiv.org/abs/1308.0374).
- [10] P. Jimenez-Delgado and E. Reya, *Phys. Rev. D* **89**, 074049 (2014).
- [11] S. Alekhin, J. Blümlein, S. Moch, and R. Placakyte, [arXiv:1508.07923](https://arxiv.org/abs/1508.07923).
- [12] A. Accardi, M. E. Christy, C. E. Keppel, P. Monaghan, W. Melnitchouk, J. G. Morfin, and J. F. Owens, *Phys. Rev. D* **81**, 034016 (2010).
- [13] A. Accardi, W. Melnitchouk, J. F. Owens, M. E. Christy, C. E. Keppel, L. Zhu, and J. G. Morfin, *Phys. Rev. D* **84**, 014008 (2011).
- [14] J. F. Owens, A. Accardi, and W. Melnitchouk, *Phys. Rev. D* **87**, 094012 (2013).
- [15] The CTEQ-Jefferson Lab (CJ) Collaboration, <http://www.jlab.org/cj>.
- [16] W. Melnitchouk and A. W. Thomas, *Phys. Lett. B* **377**, 11 (1996).
- [17] V. M. Abazov *et al.*, *Phys. Rev. D* **88**, 091102 (2013).
- [18] V. M. Abazov *et al.*, *Phys. Rev. D* **91**, 032007 (2015).
- [19] V. M. Abazov *et al.*, *Phys. Rev. Lett.* **112**, 151803 (2014); **114**, 049901 (2015).
- [20] N. Baillie *et al.*, *Phys. Rev. Lett.* **108**, 142001 (2012).
- [21] S. Tkachenko *et al.*, *Phys. Rev. C* **89**, 045206 (2014).
- [22] M. Krämer, F. I. Olness, and D. E. Soper, *Phys. Rev. D* **62**, 096007 (2000).
- [23] A. Accardi, *Mod. Phys. Lett. A* **28**, 1330032 (2013).
- [24] G. R. Farrar and D. R. Jackson, *Phys. Rev. Lett.* **35**, 1416 (1975).
- [25] F. E. Close, *Phys. Lett.* **43B**, 422 (1973).
- [26] F. E. Close and W. Melnitchouk, *Phys. Rev. C* **68**, 035210 (2003).
- [27] R. J. Holt and C. D. Roberts, *Rev. Mod. Phys.* **82**, 2991 (2010).
- [28] C. D. Roberts, R. J. Holt, and S. M. Schmidt, *Phys. Lett. B* **727**, 249 (2013).
- [29] E. A. Hawker *et al.*, *Phys. Rev. Lett.* **80**, 3715 (1998); J. Webb, Ph.D. Thesis, New Mexico State University, 2002, [arXiv:hep-ex/0301031](https://arxiv.org/abs/hep-ex/0301031).
- [30] R. S. Towell *et al.*, *Phys. Rev. D* **64**, 052002 (2001).
- [31] Fermilab E906 experiment (SeaQuest), Drell-Yan measurements of nucleon and nuclear structure with the Fermilab main injector, <http://www.phy.anl.gov/mep/SeaQuest/index.html>.
- [32] A. Accardi, F. Arleo, W. K. Brooks, D. D'Enterria, and V. Muccifora, *Riv. Nuovo Cimento* **32**, 439 (2010).
- [33] A. Majumder and M. van Leeuwen, *Prog. Part. Nucl. Phys.* **66**, 41 (2011).
- [34] K. J. Eskola, H. Paukkunen, and C. A. Salgado, *J. High Energy Phys.* **04** (2009) 065.
- [35] D. de Florian, R. Sassot, P. Zurita, and M. Stratmann, *Phys. Rev. D* **85**, 074028 (2012).
- [36] K. Kovarik *et al.*, *Phys. Rev. D* **93**, 085037 (2016).
- [37] G. Aad *et al.*, *Phys. Rev. Lett.* **109**, 012001 (2012).
- [38] S. Alekhin, J. Blümlein, L. Caminadac, K. Lipka, K. Lohwasser, S. Moch, R. Petti, and R. Placakyte, *Phys. Rev. D* **91**, 094002 (2015).
- [39] S. Catani, D. de Florian, G. Rodrigo, and W. Vogelsang, *Phys. Rev. Lett.* **93**, 152003 (2004).
- [40] A. I. Signal and A. W. Thomas, *Phys. Lett. B* **191**, 205 (1987).
- [41] G. P. Zeller *et al.*, *Phys. Rev. D* **65**, 111103 (2002); **67**, 119902 (2003).
- [42] F. I. Olness and W.-K. Tung, *Nucl. Phys.* **B308**, 813 (1988); M. A. Aivazis, F. I. Olness, and W.-K. Tung, *Phys. Rev. D* **50**, 3085 (1994); M. A. Aivazis, J. C. Collins, F. I. Olness, and W.-K. Tung, *Phys. Rev. D* **50**, 3102 (1994).
- [43] H. Georgi and H. D. Politzer, *Phys. Rev. D* **14**, 1829 (1976).
- [44] I. Schienbein *et al.*, *J. Phys. G* **35**, 053101 (2008).
- [45] L. T. Brady, A. Accardi, T. J. Hobbs, and W. Melnitchouk, *Phys. Rev. D* **84**, 074008 (2011); **85**, 039902 (2012).
- [46] O. W. Greenberg and D. Bhaumik, *Phys. Rev. D* **4**, 2048 (1971).
- [47] O. Nachtmann, *Nucl. Phys.* **B63**, 237 (1973).
- [48] R. K. Ellis, R. Petronzio, and G. Parisi, *Phys. Lett.* **64B**, 97 (1976).
- [49] A. Accardi, T. Hobbs, and W. Melnitchouk, *J. High Energy Phys.* **11** (2009) 084.
- [50] J. V. Guerrero, J. J. Ethier, A. Accardi, S. W. Casper, and W. Melnitchouk, *J. High Energy Phys.* **09** (2015) 169.
- [51] M. A. G. Aivazis, F. I. Olness, and W. K. Tung, *Phys. Rev. D* **50**, 3085 (1994).
- [52] S. Kretzer and M. H. Reno, *Phys. Rev. D* **66**, 113007 (2002).
- [53] A. Accardi and J.-W. Qiu, *J. High Energy Phys.* **07** (2008) 090.
- [54] F. M. Steffens, M. D. Brown, W. Melnitchouk, and S. Sanches, *Phys. Rev. C* **86**, 065208 (2012).
- [55] M. Virchaux and A. Milsztajn, *Phys. Lett. B* **274**, 221 (1992).
- [56] S. I. Alekhin, S. A. Kulagin, and S. Liuti, *Phys. Rev. D* **69**, 114009 (2004).
- [57] J. Blümlein and H. Böttcher, *Phys. Lett. B* **662**, 336 (2008).
- [58] J. Blümlein, *Prog. Part. Nucl. Phys.* **69**, 28 (2013).
- [59] B. Badelek and J. Kwiecinski, *Nucl. Phys.* **B370**, 278 (1992).
- [60] W. Melnitchouk and A. W. Thomas, *Phys. Rev. D* **47**, 3783 (1993).
- [61] L. P. Kaptari and A. Y. Umnikov, *Phys. Lett. B* **272**, 359 (1991).
- [62] W. Melnitchouk, A. W. Schreiber, and A. W. Thomas, *Phys. Rev. D* **49**, 1183 (1994).

- [63] S. A. Kulagin, G. Piller, and W. Weise, *Phys. Rev. C* **50**, 1154 (1994).
- [64] P. J. Ehlers, A. Accardi, L. T. Brady, and W. Melnitchouk, *Phys. Rev. D* **90**, 014010 (2014).
- [65] S. A. Kulagin, W. Melnitchouk, G. Piller, and W. Weise, *Phys. Rev. C* **52**, 932 (1995).
- [66] S. A. Kulagin and R. Petti, *Nucl. Phys. A* **765**, 126 (2006).
- [67] Y. Kahn, W. Melnitchouk, and S. A. Kulagin, *Phys. Rev. C* **79**, 035205 (2009).
- [68] R. B. Wiringa, V. G. J. Stoks, and R. Schiavilla, *Phys. Rev. C* **51**, 38 (1995).
- [69] R. Machleidt, *Phys. Rev. C* **63**, 024001 (2001).
- [70] F. Gross and A. Stadler, *Phys. Rev. C* **78**, 014005 (2008); **82**, 034004 (2010).
- [71] J. Arrington, F. Coester, R. J. Holt, and T.-S. H. Lee, *J. Phys. G* **36**, 025005 (2009).
- [72] J. Arrington, J. G. Rubin, and W. Melnitchouk, *Phys. Rev. Lett.* **108**, 252001 (2012).
- [73] F. Gross and S. Liuti, *Phys. Rev. C* **45**, 1374 (1992).
- [74] W. Melnitchouk, A. W. Schreiber, and A. W. Thomas, *Phys. Lett. B* **335**, 11 (1994).
- [75] W. Melnitchouk, M. Sargsian, and M. Strikman, *Z. Phys. A* **359**, 99 (1997).
- [76] H. Mineo, W. Bentz, N. Ishii, A. W. Thomas, and K. Yazaki, *Nucl. Phys. A* **735**, 482 (2004).
- [77] I. C. Cloet, W. Bentz, and A. W. Thomas, *Phys. Lett. B* **642**, 210 (2006).
- [78] J. J. Aubert *et al.*, *Phys. Lett.* **123B**, 275 (1983).
- [79] D. F. Geesaman, K. Saito, and A. W. Thomas, *Annu. Rev. Nucl. Part. Sci.* **45**, 337 (1995).
- [80] A. D. Martin, A. J. Th. M. Mathijssen, W. J. Stirling, R. S. Thorne, B. J. A. Watt, and G. Watt, *Eur. Phys. J. C* **73**, 2318 (2013).
- [81] A. C. Benvenuti *et al.*, *Phys. Lett. B* **223**, 485 (1989); **236**, 592 (1989).
- [82] L. W. Whitlow, E. M. Riordan, S. Dasu, S. Rock, and A. Bodek, *Phys. Lett. B* **282**, 475 (1992).
- [83] M. Arneodo *et al.*, *Nucl. Phys. B* **483**, 3 (1997).
- [84] M. Arneodo *et al.*, *Nucl. Phys. B* **487**, 3 (1997).
- [85] H. Abramowicz *et al.*, *Eur. Phys. J. C* **75**, 580 (2015).
- [86] A. Airapetian *et al.*, *J. High Energy Phys.* **05** (2011) 126.
- [87] S. P. Malace *et al.*, *Phys. Rev. C* **80**, 035207 (2009).
- [88] D. Acosta *et al.*, *Phys. Rev. D* **71**, 051104(R) (2005).
- [89] T. Aaltonen *et al.*, *Phys. Rev. Lett.* **102**, 181801 (2009).
- [90] T. Aaltonen *et al.*, *Phys. Lett. B* **692**, 232 (2010).
- [91] V. M. Abazov *et al.*, *Phys. Rev. D* **76**, 012003 (2007).
- [92] T. Aaltonen *et al.*, *Phys. Rev. D* **78**, 052006 (2008).
- [93] V. M. Abazov *et al.*, *Phys. Rev. Lett.* **101**, 062001 (2008); B. Abbott *et al.*, *Phys. Rev. Lett.* **86**, 1707 (2001).
- [94] V. M. Abazov *et al.*, *Phys. Lett. B* **666**, 435 (2008).
- [95] S. Alekhin, K. Melnikov, and F. Petriello, *Phys. Rev. D* **74**, 054033 (2006).
- [96] G. Moreno *et al.*, *Phys. Rev. D* **43**, 2815 (1991).
- [97] P. Jimenez-Delgado, T. J. Hobbs, J. T. Londergan, and W. Melnitchouk, *Phys. Rev. Lett.* **114**, 082002 (2015).
- [98] K. A. Olive *et al.*, *Chin. Phys. C* **38**, 090001 (2014).
- [99] S. Alekhin, J. Blümlein, and S.-O. Moch, *Phys. Rev. D* **86**, 054009 (2012).
- [100] L. A. Harland-Lang, A. D. Martin, P. Motylinski, and R. S. Thorne, *Eur. Phys. J. C* **76**, 186 (2016).
- [101] Jefferson Lab Experiment C12-10-103 (MARATHON), G. G. Petratos, J. Gomez, R. J. Holt, and R. D. Ransome, spokespersons.
- [102] Jefferson Lab Experiment E12-10-102 (BONUS12), S. Bültmann, M. E. Christy, H. Fenker, K. Griffioen, C. E. Keppel, S. Kuhn, and W. Melnitchouk, spokespersons.
- [103] Jefferson Lab Experiment E12-10-007 (SoLID), P. Souder, spokesperson.
- [104] A. Accardi, *Proc. Sci.*, DIS2015 (2015) 001, [arXiv:1602.02035](https://arxiv.org/abs/1602.02035).
- [105] A. D. Martin, R. G. Roberts, W. J. Stirling, and R. S. Thorne, *Eur. Phys. J. C* **35**, 325 (2004).
- [106] S. Alekhin, J. Blümlein, S. Klein, and S.-O. Moch, *Phys. Rev. D* **81**, 014032 (2010).
- [107] L. T. Brady, A. Accardi, W. Melnitchouk, and J. F. Owens, *J. High Energy Phys.* **06** (2012) 019.
- [108] A. Accardi *et al.*, [arXiv:1603.08906](https://arxiv.org/abs/1603.08906).
- [109] I. R. Afnan, F. Bissey, J. Gomez, A. T. Katramatou, W. Melnitchouk, G. G. Petratos, and A. W. Thomas, *Phys. Lett. B* **493**, 36 (2000);
- [110] I. R. Afnan, F. Bissey, J. Gomez, A. T. Katramatou, S. Liuti, W. Melnitchouk, G. G. Petratos, and A. W. Thomas *Phys. Rev. C* **68**, 035201 (2003).
- [111] E. Pace, G. Salme, S. Scopetta, and A. Kievsky, *Phys. Rev. C* **64**, 055203 (2001).
- [112] M. M. Sargsian, S. Simula, and M. I. Strikman, *Phys. Rev. C* **66**, 024001 (2002).